Revista Brasileira de Geofísica
RBGf
Brazilian Journal of Geophysics

Revista Brasileira de Geofísica (2013) 31(4): 683-697

ISSN 0102-261X
www.scielo.br/rbg

Q FACTOR ESTIMATION FROM SURFACE AND VSP SEISMIC DATA: A NUMERICAL MODELING STUDY

Adalto Oliveira da Silva, Roseane Marchezi Misságia and Marco Antonio Rodrigues Ceia

ABSTRACT. Seismic acquisition is used by the petroleum industry to identify subsurface structures that meet pre-established requirements for hydrocarbon accumulation. In mature fields, such surveys are important to monitor the reserves, the producing wells and to aid the development of projects for new wells location. This work proposes a processing workflow that seeks to improve the high frequency content of the seismic signal, which is the most attenuated part of the frequency spectrum of such kind of signal, especially in surface seismic data. The method is based on the calculation of Q factor from VSP data which allows defining an inverse Q_{ef} filter to be applied in surface seismic data. This processing flow was tested in two datasets derived from numerical models: one with plain-parallel layers and another representing the wedge type reservoir. Such numerical modeling aimed to simulate the attenuation of the seismic signal concerning the geometry and saturation effects in those two reservoir models, which allows testing the efficiency of the inverse Q_{ef} filter that was designed to mitigate energy loss effects in seismic waves used for reservoir characterization.

Keywords: attenuation coefficient, quality factor, seismic characterization, petroleum reservoir.

RESUMO. A aquisição sísmica é utilizada pela indústria do petróleo com a finalidade de identificar em subsuperfície estruturas que satisfaçam os requisitos pré-estabelecidos para acumulação de hidrocarbonetos. Em campos maduros, tais levantamentos são importantes para monitorar reservas, poços produtores e desenvolver novos projetos de poço. Nesse artigo propõe-se um fluxo de processamento voltado para o melhoramento das altas frequências atenuadas nos dados sísmicos de superfície. Isto será feito a partir do cálculo do fator Q utilizando dados sísmicos de poço para definir um filtro inverso Q_{ef} e realizar a filtragem de dados sísmicos de superfície. Este fluxo foi testado em dois conjuntos de dados provenientes de simulações numéricas: com camadas planas e paralelas, e outro com camadas inclinadas simulando a borda acunhada (wedge) de um reservatório delgado. A modelagem numérica teve como propósito simular a atenuação do sinal sísmico associado aos efeitos da geometria e saturação nos dois tipos de reservatórios, possibilitando testar a eficácia do filtro inverso Q_{ef} proposto para mitigar os efeitos da perda de energia da onda sísmica na caracterização de reservatórios de hidrocarbonetos.

Palavras-chave: coeficiente de atenuação, fator de qualidade, caracterização sísmica, reservatório de petróleo.

Laboratório de Engenharia e Exploração de Petróleo (LENEP), Universidade Estadual do Norte Fluminense Darcy Ribeiro (UENF), Rod. Amaral Peixoto, km 163, s/n, Imboacica, 27925-310 Macaé, RJ, Brazil. Phone: +55(22) 2765-6564 – E-mails: adaltoos@bol.com.br; rose@lenep.uenf.br; marco@lenep.uenf.br

INTRODUCTION

The estimate of the Q factor has been studied by several researchers (Hargreaves & Calvert, 1991, Guerra & Leaney, 2006; Yang & Gao, 2010; Quintal et al., 2009, 2011; Blias, 2012; Reine et al., 2012) due to its importance as a tool for reservoir characterization. It can restore the high frequency range of seismic reflection data aiming at improving the resolution of seismic data (Raji & Rietbrock, 2011), identifying important attributes and interpreting small-scale seismic stratigraphic features (Chopra et al., 2004) and work as a direct indicator of hydrocarbons (Castagna et al., 2003).

Several techniques have been proposed to enhance the knowledge and increase the reliability of this seismic attribute. The Q factor can be estimated by CMP data, but the accuracy is drastically reduced (Wang, 2002). The calibration of surface data by seismic well has an important advantage, since it allows including the inelastic absorption effect. Tonn (1991) compared several methods to estimate the Q factor through VSP (Vertical Seismic Profile) data and argues that their performance is directly related to the preservation of amplitude and noise level of the seismic data. Bath (1974) indicated the spectral ratio method for estimating the Q factor since it does not need true-amplitude seismic data.

In this work, we propose a processing flowchart for inverse Q_{ef} filter (Q effective) aimed at increasing the amplitude and restoring the frequency of the surface seismic signal, using for this purpose the interface Q_{ef} factor. The proposal includes replacing in the filter, the constant Q factor for a Q_{ef} factor that represents accurately the attenuation of seismic waves in each layer. It was also considered using an interpolating polynomial that allows filtering each seismic trace using its Q_{ef} factor. Filter stability is analyzed using a function proposed by Wang (2002).

The numerical simulation of the P-wave propagation aimed at faithfully reproducing the attenuation and Q factor effects, and subsequent improvement of frequency in two sets (VSP and surface data) recorded in the models: wedge, as well as flat and parallel layers, both representatives of top and base structural features present in oil reservoirs.

METHODS

The seismic pulse loses energy during the propagation through the Earth interior, due to the effects of absorption, scattering and spherical divergence. Attenuation is an important physical property of sedimentary rocks saturated with hydrocarbons, and is often not considered in the characterization procedures with surface seismic data (Yang et al., 2009). The estimate of the absorption coefficient or factor Q using seismic data reveals useful information, such as: lithology, degree of saturation of the rock and presence of fluids in the pores, porosity, permeability (Carcione & Picotti, 2006; Picotti et al., 2007), and indicate porosity and saturation heterogeneity as the most severe mechanism of decaying amplitude. That justifies the importance of incorporating the attenuation effects in the evaluation of reflection coefficients to improve the resolution of images and minimize the impact on the amplitude variation offset (AVO), which substantially affects the post-critical reflections (Chopra et al., 2004).

The Q factor is a parameter used to characterize the attenuation in an inelastic medium, which is defined as the ratio between the energy of the seismic signal and the energy lost in each cycle.

Barton (2007) found that the laboratory attenuation may be approximated linearly to frequency, i.e., the attenuated signal may be considered as a linear combination of the attenuated components. Therefore, the higher frequency components of the seismic pulse suffer more the attenuation effects than the lower frequency components, resulting in loss of resolution of the seismograms. The constant Q model, which has been commonly adopted due to the linearity assumption (Kjartansson, 1979; Tonn, 1991), is a good guess when the attenuation coefficient is not extremely high ($Q > 10$). The sensitivity of the attenuation to changing signal frequency, phase and amplitude makes the VSP data more accurate to estimate the Q factor. The VSP geometry considers that the seismic wave travels only once through the inelastic medium; therefore, the VSP data contain higher frequencies and higher signal/noise ratio when compared to surface seismic data.

The analytical expression of the amplitude attenuation of the seismic signal can be given by (Aki & Richards, 1980):

$$A(\omega) = A_0(\omega)e^{-\alpha x} = A_0(\omega)e^{\left[-\frac{\omega(t-t_0)}{2Q}\right]} \qquad (1)$$

where $A(\omega)$ and $A_0(\omega)$ are the spectra of the amplitudes of the seismic signal recorded in the receiver at two subsequent depths. The expression $\alpha = \frac{\pi f}{QV}$ is the attenuation coefficient; f, the wave frequency; V, velocity; and Q, the layer quality factor.

When including $\omega = 2\pi f$ in Eq. (1):

$$A(t, f) = A_0(t_0, f)e^{-\frac{\pi f(t-t_0)}{Q}}\,. \qquad (2)$$

From Eq. (2) we obtain:

$$\ln\left(\frac{A(t, f)}{A_0(t_0, f)}\right) = \frac{\pi f(t - t_0)}{Q}\,. \qquad (3)$$

In Equation (3), t and t_0 are the arrival times at two subsequent depths and represent the amplitude decay of the seismic signal.

Using Equation (3) to express the Q factor:

$$Q = -\frac{\pi f(t-t_0)}{\ln\left(\frac{A(t,f)}{A_0(t_0,f)}\right)}$$

$$\frac{\ln\left(\frac{A(t,f)}{A(t_0,f)}\right)}{f} = -\frac{\pi(t-t_0)}{Q}$$

$$Q = -\pi f(t-t_0) \times \left(\ln\left(\frac{A(t,f)}{A_0(t_0,f)}\right)\right)^{-1} \quad (4)$$

$$\frac{1}{Q} = -\frac{\ln\left(A(t,f)/A_0(t,f)\right)}{\pi f(t-t_0)}$$

The spectral ratio method

This method is based on the definition of the amplitude spectra of two reference waves recorded at receivers positioned at different depths. Using this method from the VSP data is a useful technique to estimate seismic amplitude attenuation (Tonn, 1991). This concept is summarized in Figure 1 (A, B, C). Figure 1(A) shows the first arrivals $g_1(t)$ and $g_2(t)$ registered in Z_1 and Z_2; (B) shows the spectra of amplitude $\times$ frequency $G_1(f)$ and $G_2(f)$ of $g_1(t)$ and $g_2(t)$; and, (C) shows the ratio of spectral amplitudes observed in (B).

The procedure for estimating the attenuation coefficient and the Q factor of the spectral ratio method is shown below:

1. Calculation of amplitude *versus* frequency spectra;
2. Computing the ratio of two spectra of reference wave amplitude;
3. Linear adjustment (least squares) of the ratio amplitude $\times$ frequency spectra of two functions;
4. Obtaining the slope of the line (slope):

$$\text{slope} = \frac{\ln\left(\frac{A(t,f)}{A(t_0,f)}\right)}{f}, \quad (5)$$

5. Obtaining the amplitude decay time: $\tau = t - t_0$;
6. Writing Equation (5) as a function of the slope and the Q factor:

$$\text{slope} = -\frac{\pi(t-t_0)}{Q}$$

$$Q = -\frac{\pi\tau}{\text{slope}}. \quad (6)$$

Effective Q factor

The use of the inverse Q filter for improving the seismic resolution and true amplitude processing requires reliable models to estimate the Q factor of the layers. Such models consider the amplitude loss of the seismic signal for the route between source and receiver. The Q factor of the layers can be accurately estimated by the zero offset VSP acquisition in the vicinity of the well. Guerra & Leaney (2006) developed a theoretical method, which combines measurements based on zero offset VSP, walkway or CMP families acquisitions, arguing that for small source-receiver offsets the Q_{ef} factor approaches a weighted harmonic average of Q-factor values of each layer, according to Equation (7) that returns the Q_{ef} factor for small offsets in the depth z_n.

$$p \to 0 (x_p \to 0) : Q_n^{ef}(x_p) = \frac{\sum_{k=1}^{n} \Delta t_k V_k^2}{\sum_{k=1}^{n} \frac{\Delta t_k V_k^2}{Q_k}}. \quad (7)$$

Here Δt_k is the transit time at zero offset VSP; V_k, the interval velocity; $\langle Q_n^{ef} \rangle$ the harmonic mean of the Q factor values in layer k; $\Delta t_k V_k^2$, the weighting factor; p is the parameter of the radius, and x is the distance between the source and well.

On an inclined surface the transit time of the seismic wave is not the same for each reflection point in the subsurface. This requires introducing a polynomial interpolation in the algorithm that estimates the Q_{ef} factor for each point of the interface. Thus, given $(n+1)$ distinct points $x_0, x_1, \ldots, x_n$ and $Q_{ef}(x)$ factor values for these points, it is possible to approximate the $Q_{ef}(x)$ using a $p_n(x)$ polynomial of degree less than or equal to n, such as:

$$Q_{ef}(x_i) = p_n(x_i), \qquad \text{for } i = 0, 1, 2, \ldots, n. \quad (8)$$

From the Lagrange polynomial, when $p_n(x_i) = y_i$, we have:

$$p_n(x_i) = y_0 L_0(x_i) + y_1 L_1(x_i) + \cdots + y_n L_n(x_i)$$

$$p_n(x) = \sum_{k=0}^{n} y_k L_k(x)$$

where,

$$L_k(x) = \frac{\prod_{\substack{j=0 \\ j\neq k}}^{n} (x - x_j)}{\prod_{\substack{j=0 \\ j\neq k}}^{n} (x_k - x_j)} \quad (9)$$

Rewriting Equation (8) as a function of $p_n(x)$:

$$Q_{ef}(x) = \sum_{k=0}^{n} y_k L_k(x) \quad (10)$$

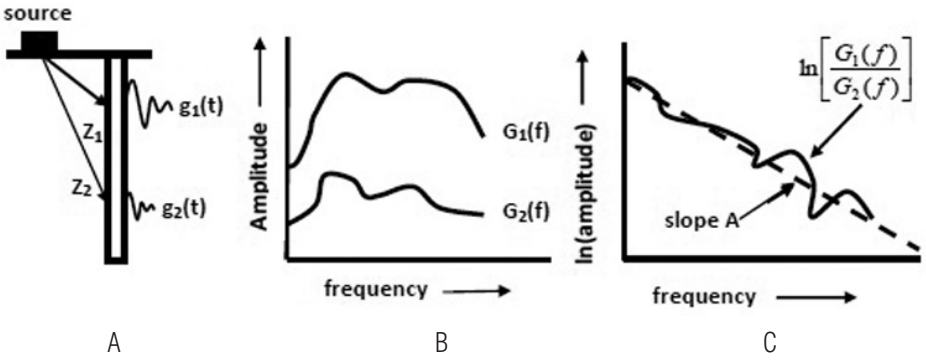

Figure 1 – Concept illustration of seismic amplitude attenuation by the spectral ratio method. Adapted from Hardage (2000).

Considering the top and base interfaces as flat and inclined, the interpolation at $(x_0, Q_{ef}(x_0))$ and $(x_1, Q_{ef}(x_1))$ yields:

$$p_1(x) = y_0 L_0(x) + y_1 L_1(x)$$

$$L_0 = \frac{(x - x_1)}{(x_0 - x_1)}$$

$$L_1 = \frac{(x - x_0)}{(x_1 - x_0)}$$

Replacing the terms L_0 and L_1 in Equation (9) gives:

$$p_1(x) = y_0 \frac{(x - x_1)}{(x_0 - x_1)} + y_1 \frac{(x - x_0)}{(x_1 - x_0)}$$

which can be rewritten as:

$$p_1(x) = \frac{(y_1 - y_0)x}{(x_1 - x_0)} + \frac{(y_0 x_1 - y_1 x_0)}{(x_1 - x_0)} \qquad (11)$$

From Equation (9) is possible to obtain $Q_{ef}(x)$, Eq. (11), at any point of a flat and inclined interface.

$$Q_{ef}(x) = \frac{(y_1 - y_0)x}{(x_1 - x_0)} + \frac{(y_0 x_1 - y_1 x_0)}{(x_1 - x_0)} \qquad (12)$$

Inverse Q filter

The effect of attenuation worsens the resolution of the seismic data, dramatically damaging seismic interpretation. By quantifying Q_{ef}, an inverse Q filter can be deduced to recover the high frequency components of the seismic signal.

Let the amplitude spectrum of the inverse Q filter be (Yilmaz, 2001):

$$P(\tau, f) = e^{(\pi f \tau)1/Q} \qquad (13)$$

Equation (12) is used to minimize the attenuation effect caused by the exponential term in Equation (1), which written according to $\tau = t - t_0$ and the Q_{ef}, (Eq. (7)), gives the attenuated amplitude spectrum:

$$A(\tau, f) = A_0(t_0, f) e^{-(\pi f \tau)1/Q_{ef}} \qquad (14)$$

Stability of the inverse Q filter

Equation (13) consists of an exponential gain which depends on time, frequency and Q_{ef}. It is usual to set a limit for this function due to the occurrence of numerical instability caused by this gain application. This can be done by Eq. (14):

$$A_c(\tau, f) = \begin{cases} e^{(\pi \tau f)1/Q_{ef}} & \text{if } f \leq f_c\,, \\ e^{(\pi \tau f_c)1/Q_{ef}} & \text{if } f > f_c\,, \end{cases} \qquad (15)$$

where $f_c = \frac{Q_{ef}}{\pi \tau}$ is the cutoff frequency.

Applying $A_c(\tau, f)$ in Equation (13), we obtain the stability function for a cutoff frequency:

$$B_c(\tau, f) = A_c(\tau, f) A(\tau, f)\,.$$

Otherwise, the method of Wang (2002) that relies on the damping operator to propose the function $A_e(\tau, f)$ for stabilizing the exponential gain is described below:

$$A_e(\tau, f) = \frac{\beta(\tau, f) + \sigma^2}{\beta^2(\tau, f) + \sigma^2}\,,$$

where $\beta(\tau, f) = e^{\left[-\left(\frac{\pi f \tau}{Q_{ef}}\right)\right]}$ and σ^2 is a small positive constant. After this, the Q_{ef} factor is inserted into the equation to replace the constant Q used by Wang (2002).

Figure 2 compares the operators of the inverse Q filter obtained after restricting the exponential gain using the cutoff frequency and Wang (2002) stabilization function, blue and green lines, respectively.

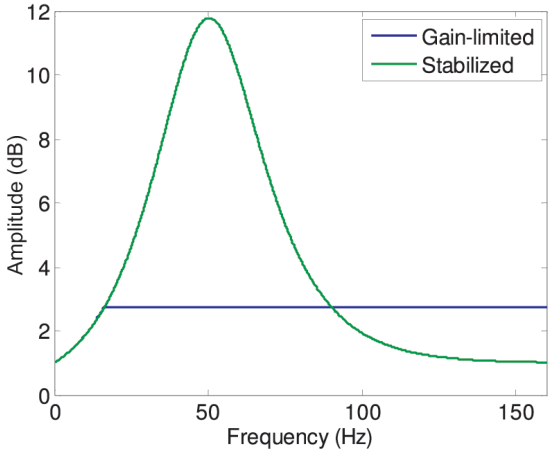

Figure 2 – Inverse Q filter for $Q = 100$: (blue) gain limited by the cutoff frequency, (green) stabilization function. Modified from Wang (2002).

Inverse Q filtering

In inverse Q filtering the goal is to eliminate the non-stationary seismic signal characteristics generated by the attenuation effect of seismic amplitude during wave propagation through the inelastic medium. In this case, the seismic waves experience some distortion: reduced amplitude, changed waveform due to the absorption of high frequency content, and phase delay. This function represents an important step in the processing flowchart that aims to improve the resolution of the seismic image. The VSP and surface data are integrated at this processing stage. The proposed inverse Q filter is applied to surface seismic data as follows: surface data acquisition, regions of interest selection and inverse Q filtering of the selected data.

Likewise, by applying $A_e(\tau, f)$ in Equation (13), the amplitude spectrum of the data $B_e(\tau, f)$ is obtained:

$$B_e(\tau, f) = A_e(\tau, f)A(\tau, f)\,. \tag{16}$$

Applying the inverse Fourier transform (IFFT) to $B_e(\tau, f)$, the operator to restore the signal amplitude is given by:

$$a(t) = \frac{1}{\pi}\int B_e(\tau, f)df\,. \tag{17}$$

NUMERICAL MODELING

To implement and validate the proposed methodology for inverse Q filtering, two sets of synthetic seismic data were used, both produced by numerical simulation of the P wave.

Equation (17) describes the unilateral pulse and causal of Berlage (Fig. 3) used in these numerical simulations:

$$w(t) = Ae^{-\alpha t^2}\sin(2\pi ft + \phi)\,. \tag{18}$$

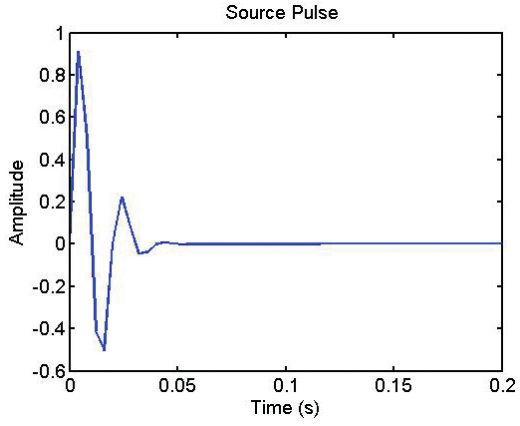

Figure 3 – Pulse Berlage used as source pulse.

Model 1, Figure 4 consists of three flat, parallel layers. The values of P-wave propagation velocity and density are specified in Table 1. The layers (R1) and (R3) represent the characteristic speed of shales. Region R2 simulates a sandstone reservoir saturated with oil. The numerical simulation of this model aims to investigate the impact of fluid saturation on the attenuation of seismic amplitude.

Table 1 – Parameters of Model 1.

Regions	Vp (m/s)	ρ (g/cm^3)
R1	2650	2270
R2	2036	1990
R3	3200	2530

Figure 4 also shows the pattern for VSP acquisition, defined based on the following parameters: source (*) – *zero offset*, depth receptor (∇) – $r_1 = 200$ m, $r_2 = 250$ m, $r_3 = 950$ m, $r_4 = 1000$ m.

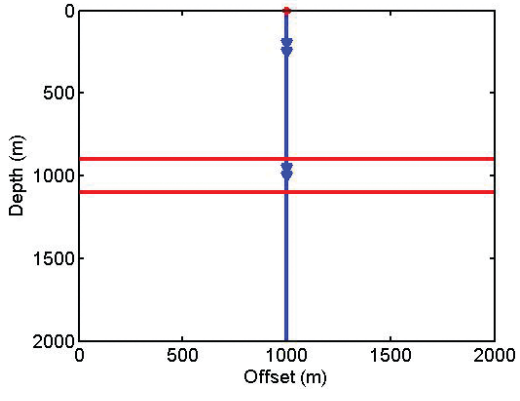

Figure 4 – Model 1 (flat and parallel layers) and VSP acquisition geometry. Adapted from Matsumura (2006).

Figure 5 shows the amplitude spectrum *versus* time of trace 50 of Model 1 seismogram, used to estimate the Q factor of the

spectral ratio method. There are reflectors delimiting the top and bottom of the reservoir, the transit time required for the displacement of the seismic waves between the source and receiver, taking into account the geometry of the VSP acquisition. The attenuation of seismic amplitude present at the top and base interfaces of the reservoir layer saturated with oil can also be observed.

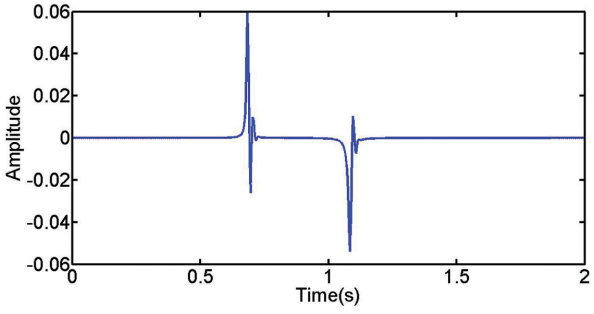

Figure 5 – Spectrum amplitude x time of trace 50 of Model 1.

Model 2, Figure 6, represents the edge of a thin wedge-shaped reservoir saturated with oil. Table 2 shows the parameters used in the simulation. The acquisition geometry used in the data survey (VSP zero offset), Figure 6, on this model has the following parameters: source (*) located on the surface; receptors (∇) located at 200, 250, 1110, 1150, 1490, 1510 m depth in the well.

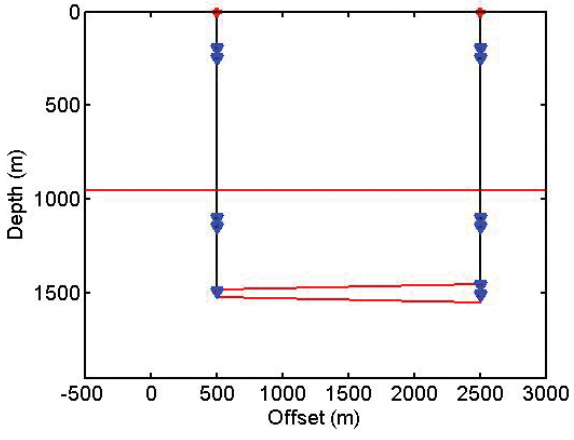

Figure 6 – Illustration of VSP geometry used on the Model 2.

Table 2 – Parameters of Model 2.

	Regions	Vp (m/s)	ρ (g/cm^3)
Water	R1	1494	0.99
Sandstone	R2	2777	1.80
Oil	R3	1690	0.86
Sandstone	R4	2777	1.80

Figure 7 shows the amplitude spectrum *vs.* time of traces 1 and 80, removed from the thinner and thicker regions of the seismogram of Model 2, respectively. Note the presence of the reflector defining the interfaces of the water depth and model top, reservoir top and bottom, and the difference between the transit times of the second and third reflection, showing the difference in the thickness of the layer between these traces, and the effect of inelastic attenuation.

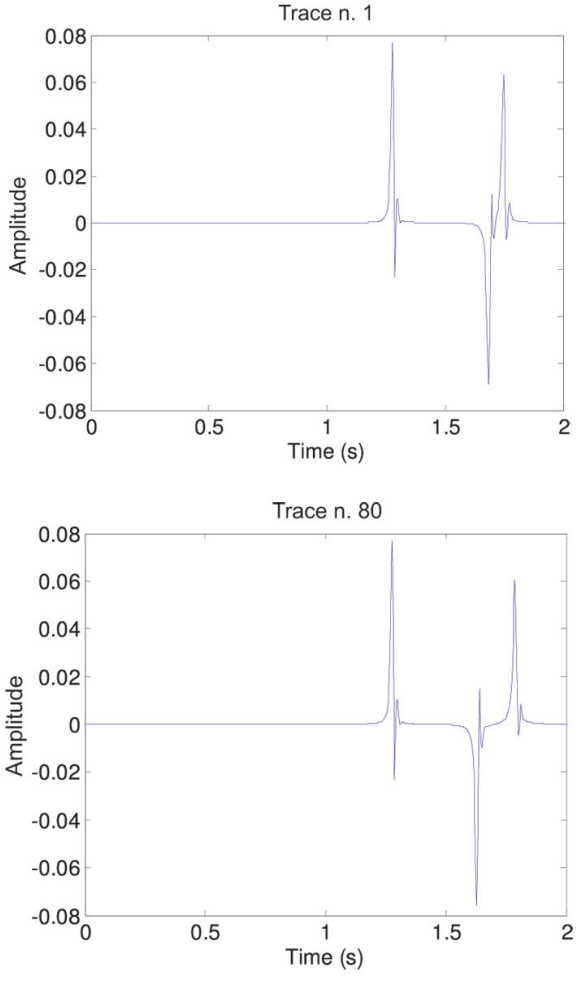

Figure 7 – Trace 1 (top) and 80 (bottom) of the seismogram of Model 2.

RESULTS

The results from the seismic numerical modeling reflect the proposed process flowchart, in which the factors Q and Q_{ef} that enable the proposition of the inverse Q_{ef} filter are defined by the VSP data, and in the next step are applied to surface seismic data to restore the frequency content of the seismic signal.

The numerical modeling performed with Models 1 and 2 demonstrate the efficiency of the proposed methodology for estimating the factor Q from VSP data presented in Tables 1, 2, 3 and 4. In Figure 8, Model 1, it is noticed that the linearity achieved

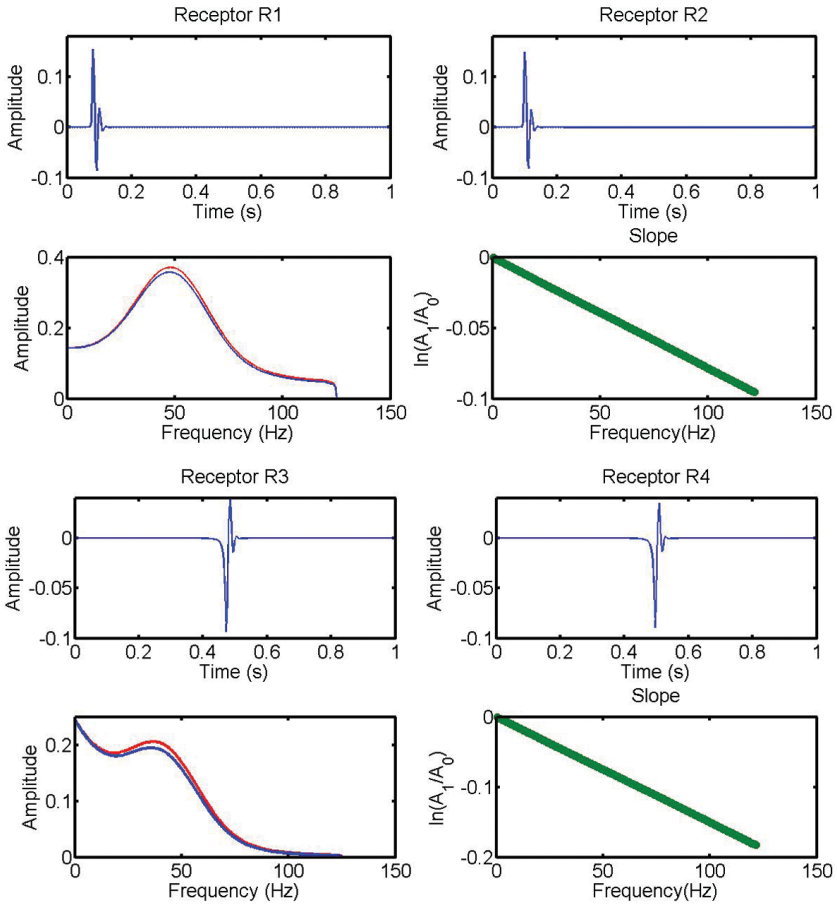

Figure 8 – Estimation of the Q factor the 1st and 2nd layers – spectral ratio method.

between the spectral ratios of the amplitudes over the range of frequencies, contributed to the accuracy of the estimate. Such behavior is expected in a numerical model of planar layers and low noise. This figure also shows two reference seismic traces, frequency spectrum, the ratio of the amplitude spectra, in addition to the linear adjustment interval that allows obtaining the slope. The changes of the waveform and amplitude attenuation are clearly seen on the analyzed results. Despite this it was possible to find the range of linearity required by the spectral ratio method and define the Q factor of the oil saturated layer.

Table 3 allows us to analyze the relationship between the Q factor of reference, estimated and effective. Note that the difference between the estimated and actual values with the reference is small, due to the linear adjustment reached between the logarithms of the amplitude spectral ratio across the frequency range. Also, the Q_{ef} obtained is greater than Q_{est} in region R2, because according to the Eq. (7), the Q_{ef} factor is a weighted harmonic average of the values of the interval Q factor, with respect to the interface considered.

Table 3 – Reference Q factor, estimated and effective for Model 1.

Regions	$Q_{reference}$	$Q_{estimated}$	$Q_{effective}$
R1	80	80.2	80.2
R2	50	50.2	73.7
R3	100	100.0	85.0

The inverse Q_{ef} filtering values were achieved using the Q_{ef} factor for each trace while a comparative analysis was performed between the seismograms before and after filtering. The result of applying this filter to the seismograms shown in the upper Figure 9 can be seen in the lower Figure 9, showing that the effect of the stabilization function promoted further improvement of the amplitudes at the base of the reservoir.

Figure 10 shows the frequency spectrum *vs.* time obtained by Gabor transform, it can be noted an increase in the frequency content around the dominant frequency (50Hz) in the filtered data both at the top and bottom of the reservoir, proportional to the presence of this attribute before filtering. Figures 11 and 12 provide an individualized analysis of these interfaces, and cor-

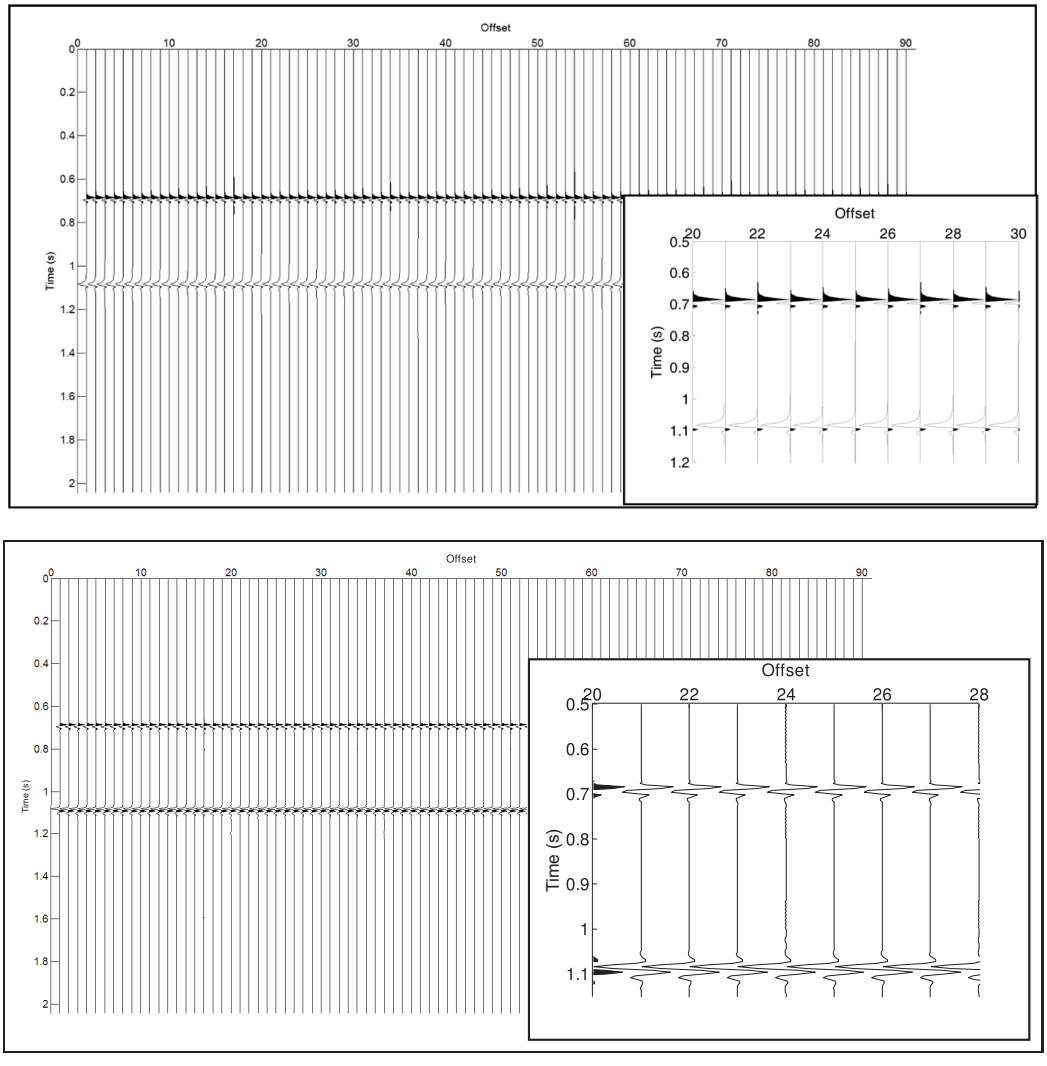

Figure 9 – Model 1 – original (top) and filtered (bottom) data.

roborate the above statement in relation to the improvement of the frequency content and amplitude restoration, verified by the joint analysis of the layers (Fig. 9).

The comparison of Q_f and Q_{ave} of Model 1 shows that the inverse filtering was more effective at the base of the oil saturated reservoir when using Q_{ef}. This has been attributed to the fact that Q_{ave} is the arithmetic average of the Q factor interval. It is noteworthy the increase of the filtered signal amplitude in both Q_{ef} and Q_{ave} compared to original data (Fig. 13).

The effectiveness of the proposed methodology can also be seen in Model 2, Figure 14 and Table 4.

Figure 14 shows the estimated Q factor interval for Model 2, considering the oil saturated model. In each of the reservoir layer of interest, two receivers are inserted as shown in Figure 6. This model also provided a good linear relationship between attenuation and frequency along almost the entire spectrum, thus improving the estimates precision of Q for each layer.

Table 4 shows the relationship between Q factor of reference, estimated and actual for Model 2.

Table 4 – Reference Q factor, estimated and effective for Model 2.

Regions	$Q_{reference}$	$Q_{estimated}$	$Q_{effective}$
R1 – Water	100	100.0	100.4
R2 – Sandstone	200	200.7	134.5
R3 – Oil	50	50.2	130.5
R4 – Sandstone	200	200.0	200.0

The calculation of the Q_{ef} on inclined layers justifies the use of an interpolating polynomial (Eq. (11)), for the top and

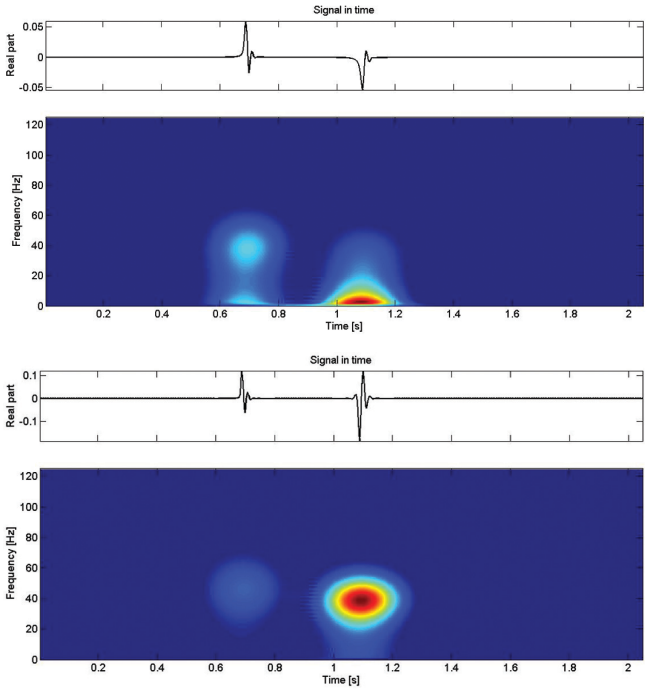

Figure 10 – Spectrogram of Model 1 – original (top) and filtered (bottom) data.

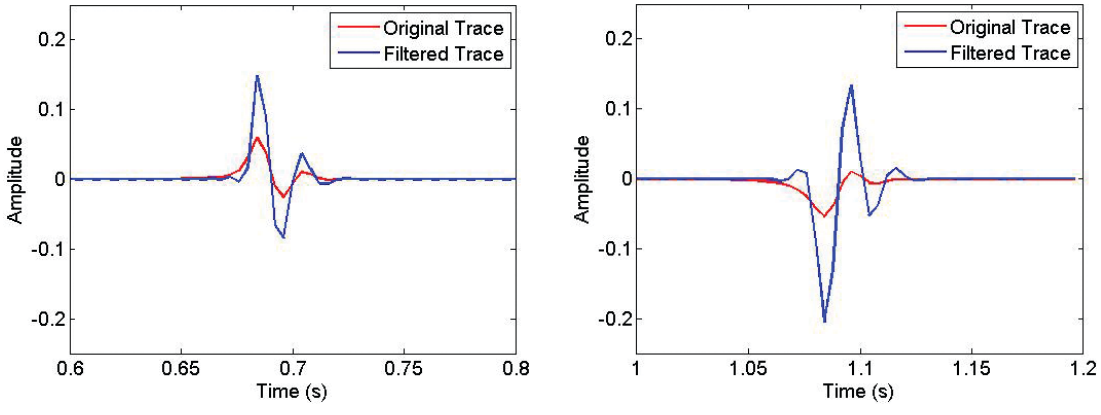

Figure 11 – Inverse Q_{ef} filtration at the top (left) and base (right) of the reservoir.

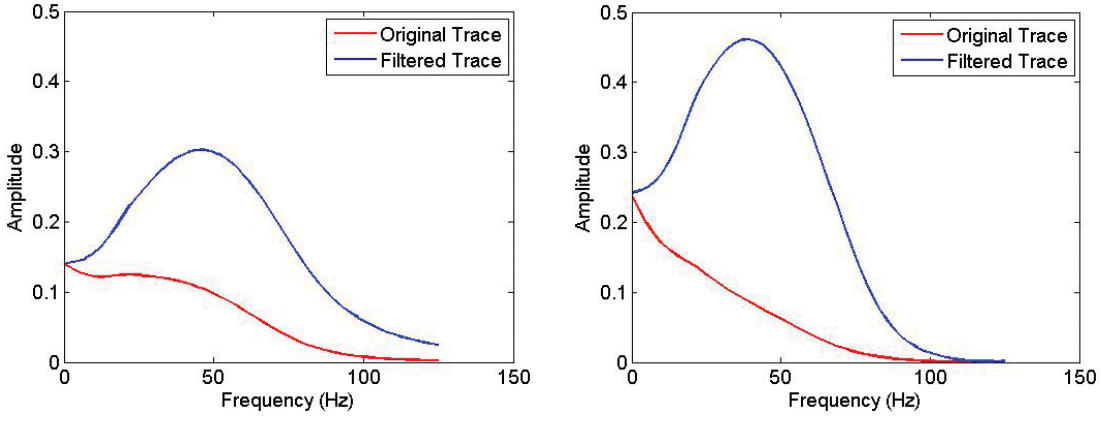

Figure 12 – Spectrum amplitude versus frequency – original and filtered data at the top (left) and base (right) of the reservoir.

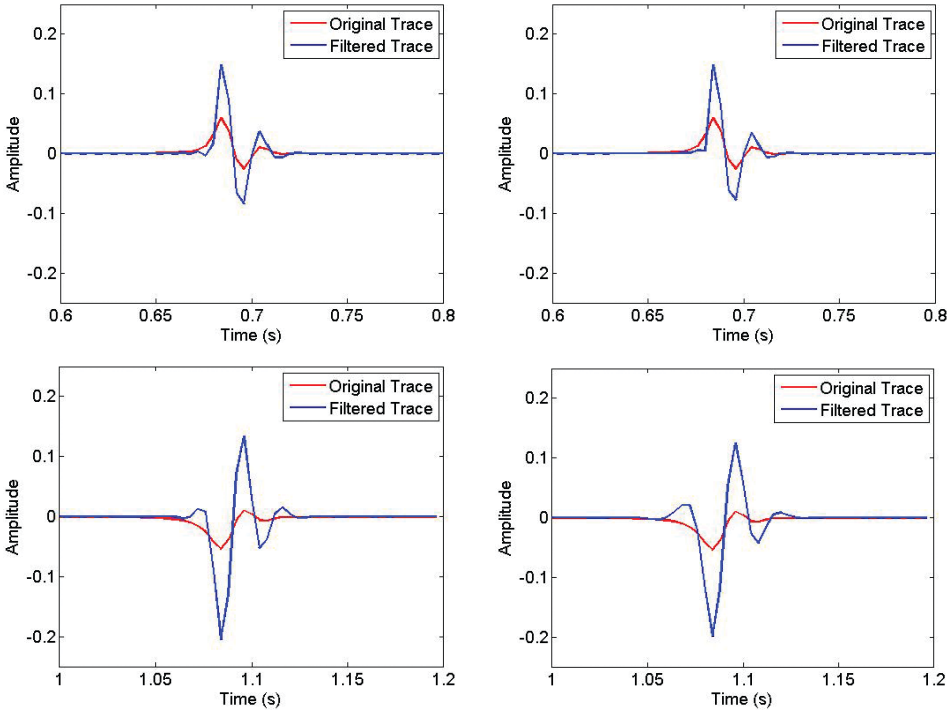

Figure 13 – Interfaces of Model 1: at the top $Q_{ef} = 80.2$ and $Q_{ave} = 65.2$ (upper); at the base $Q_{ef} = 73.7$ and $Q_{ave} = 65.2$ (bottom).

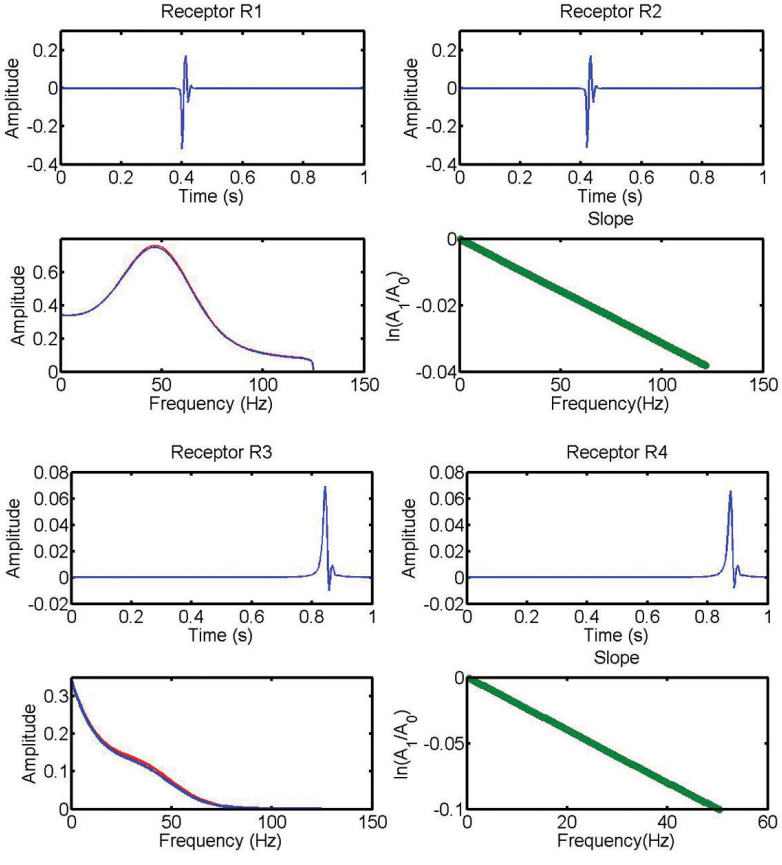

Figure 14 – Estimation of the Q factor for the 2nd and 3rd layers of Model 2.

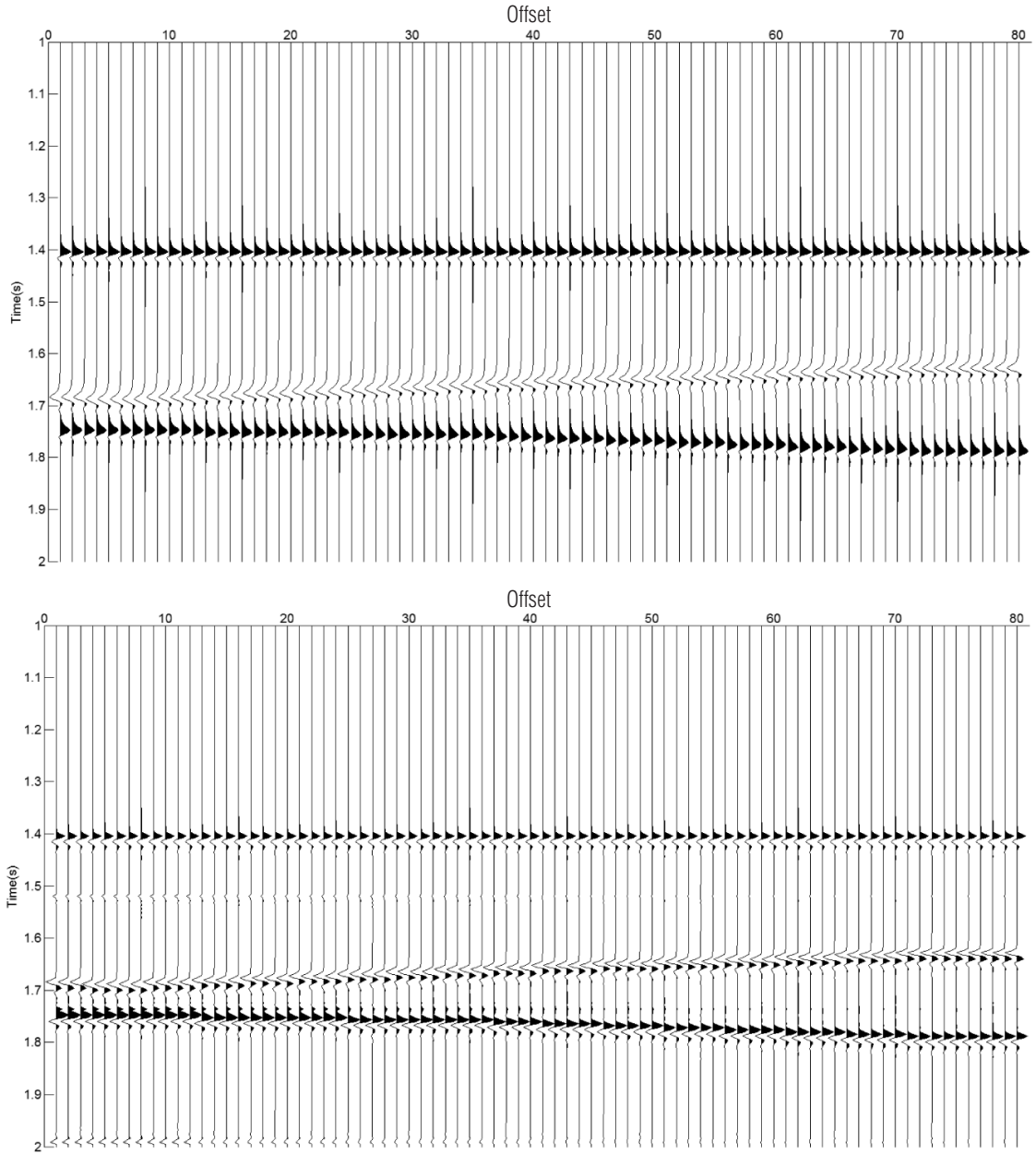

Figure 15 – Seismogram of Model 2: Original (top), filtered (bottom).

bottom interfaces of the wedge reservoir (Model 2), $Q_{ef}(x) = 0.0153\,x + 133.32$ and $Q_{ef}(x) = 0.086\,x + 123.65$, respectively. This procedure allowed to estimate a Q_{ef} for each seismogram trace, required to implement the inverse Q_{ef} filtering.

The result of this filtering applied to the surface seismic data of upper Figure 15 can be seen in the lower Figure 15, where it is noteworthy that the stabilization function performed better at the top of the reservoir (Fig. 16). This also reflects a stable behavior of the Q_{ef} values proposed within the validity range of (guess/hypothesis) of the constant Q factor.

In Figures 17-21, the plots for frequency spectrum *vs.* time obtained by Gabor transform and spectrum amplitude versus time for all interfaces show an increase in noise around the dominant frequency (50 Hz) in the filtered data, both at the reservoir top and base.

The performance of the inverse Q filtering using Q_{ef} and Q_{ave} was analyzed for trace 80 of Model 2, (Figs. 22 and 23), situated on the thick edge of the reservoir. On the interface top

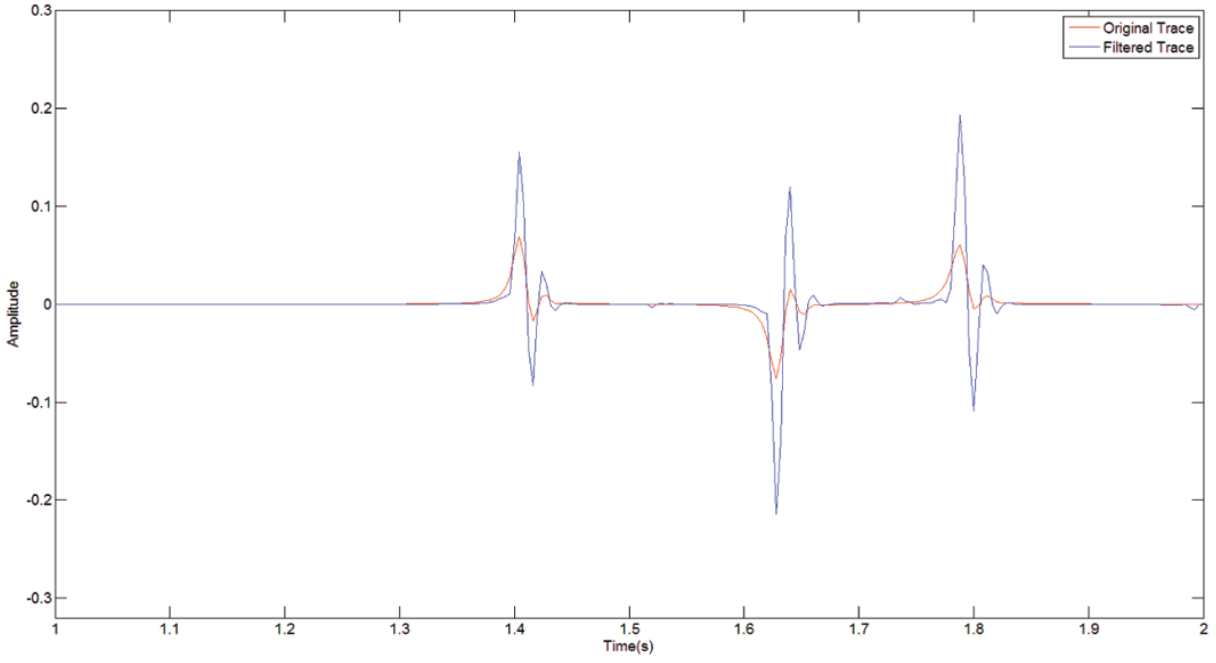

Figure 16 – Inverse Q_{ef} Filtering of seismogram – Model 2.

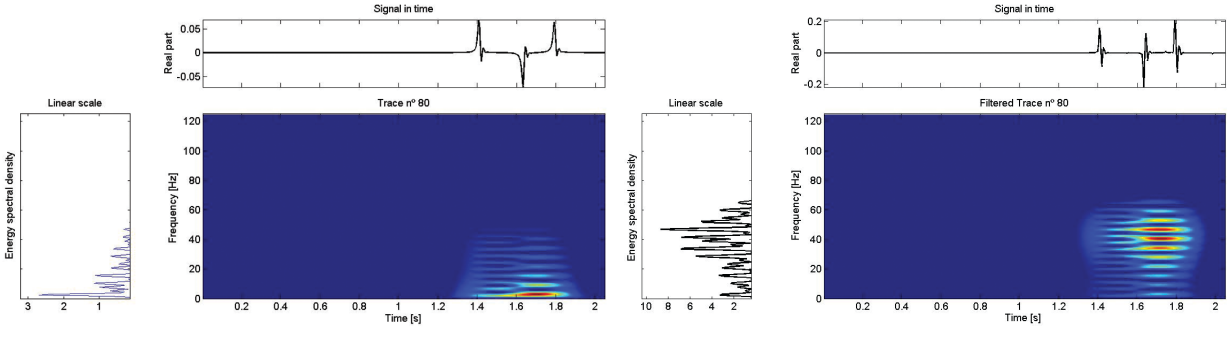

Figure 17 – Spectrogram of Model 2: original (left) and filtered (right) data.

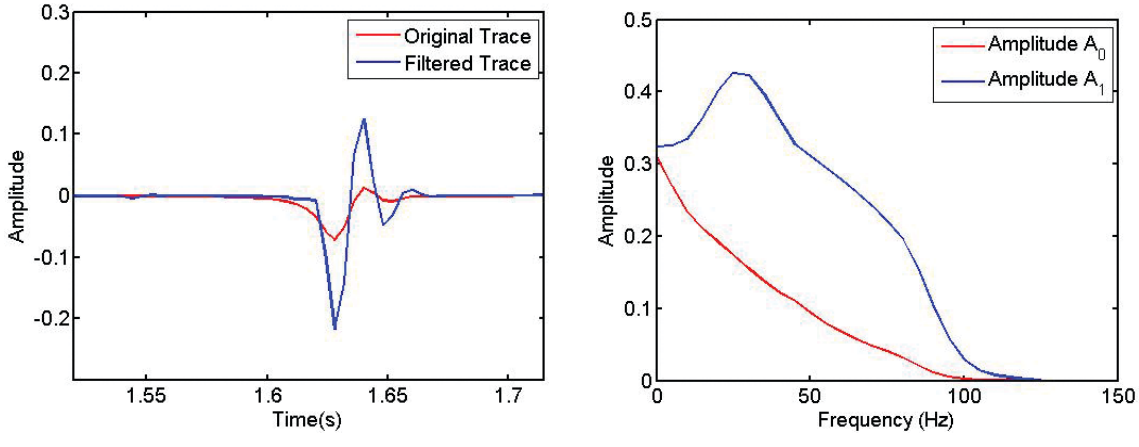

Figure 18 – Inverse Q_{ef} Filtering – Top of reservoir (Model 2).

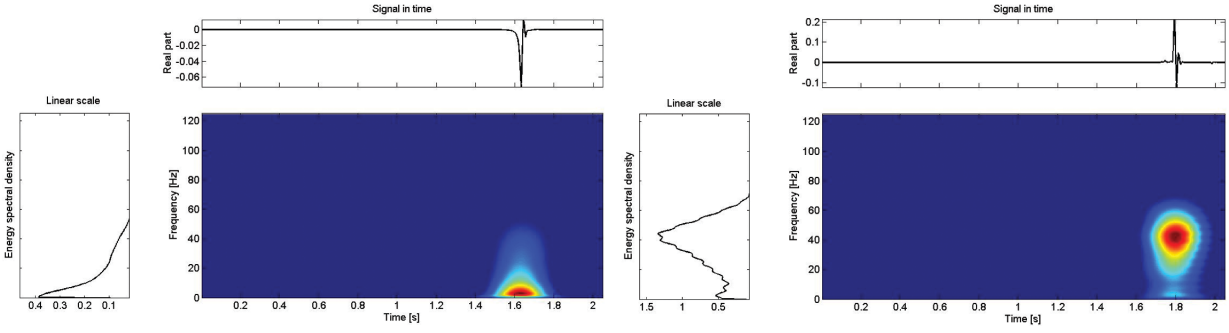

Figure 19 – Spectrogram – Top of reservoir (Model 2).

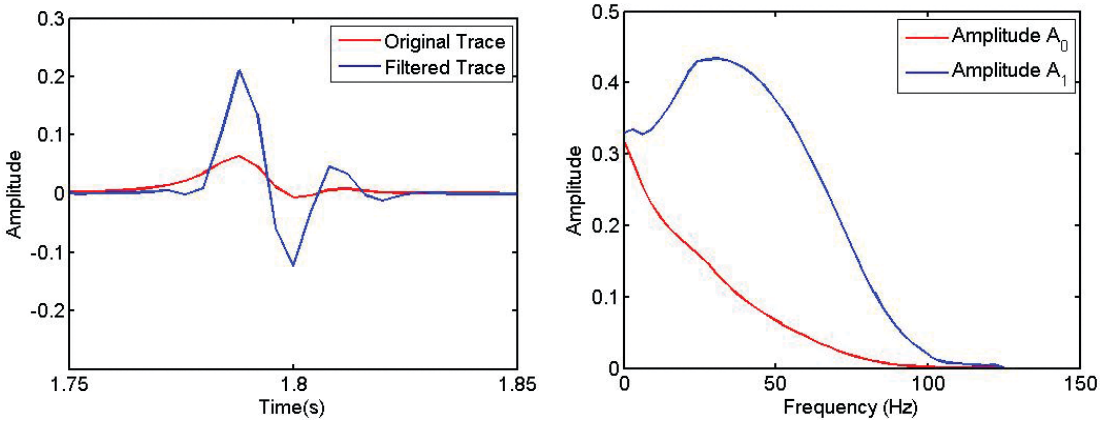

Figure 20 – Inverse Q_{ef} Filtering – Base of reservoir (Model 2).

and base, a large portion of the energy of the filtered signal is recovered. Nevertheless, it is possible to observe along each trace a deterioration of the solution as transit time of the seismic signal increases.

CONCLUSIONS

Most studies on improving the seismic data frequency spectrum using inverse filtering use a constant Q factor to filter the traces, excluding the impact of the inelastic attenuation. However, the true amplitude seismic processing requires more reliable estimates of the Q factor to improve the resolution of the seismograms.

This article proposes a processing flowchart for improving the frequency content of the seismic signal, achieving satisfactory results. The application of this procedure in the numerical modeling allowed an analysis of the different reservoir structures and stressed the important contribution of VSP data for the calculation of the Q factor of the layer, in addition to demonstrating the effectiveness of applying the spectral ratio method. The results show a small difference between the estimated value and the input parameter due to the good linear fit achieved between the spectral ratio of the amplitudes of two seismic pulses and along the frequency band.

The inverse Q_{ef} filtering proposed, modified from Guerra & Leaney (2006), contributed to a significant recovery of the frequency content in relation to Q_{ave}. The Wang (2002) function provided high stability of the inverse filtering using both Q_{ef} and Q_{ave}. In practice, what differentiates these filters is that unlike Q_{ave}, the Q_{ef} requires the selection of the intervals of interest through time windows.

Currently, several studies use numerical modeling to analyze the sensitivity of the seismic response in different geological settings. The present work studied the numerical modeling to simulate subsurface structures, parameters and saturation mode. The peculiarity of Model 2, which represents the edge of a thin wedge-reservoir, is having slanted top and bottom layers, so the inverse Q_{ef} filtering used a polynomial to interpolate and filter each seismic trace with its respective Q_{ef} factor. Because the layers of Model 1 are flat and parallel, it was possible to use a constant Q_{ef} throughout the entire interface.

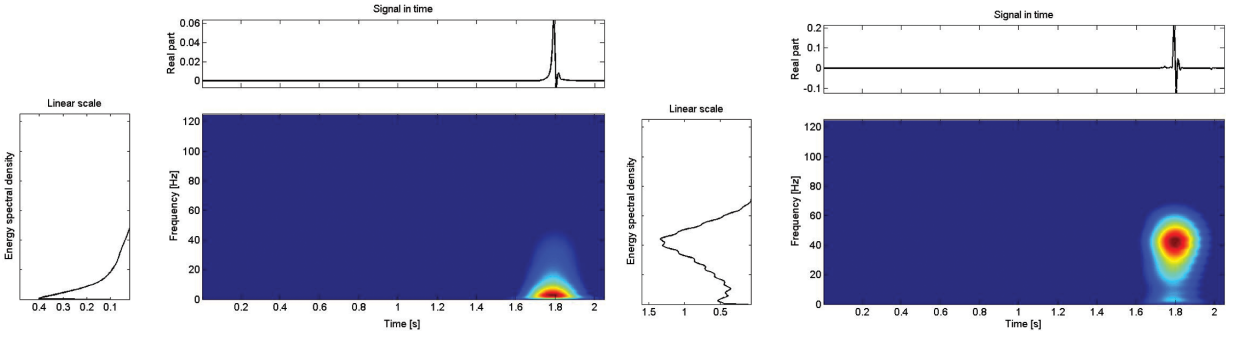

Figure 21 – Spectrogram – Base of reservoir (Model 2).

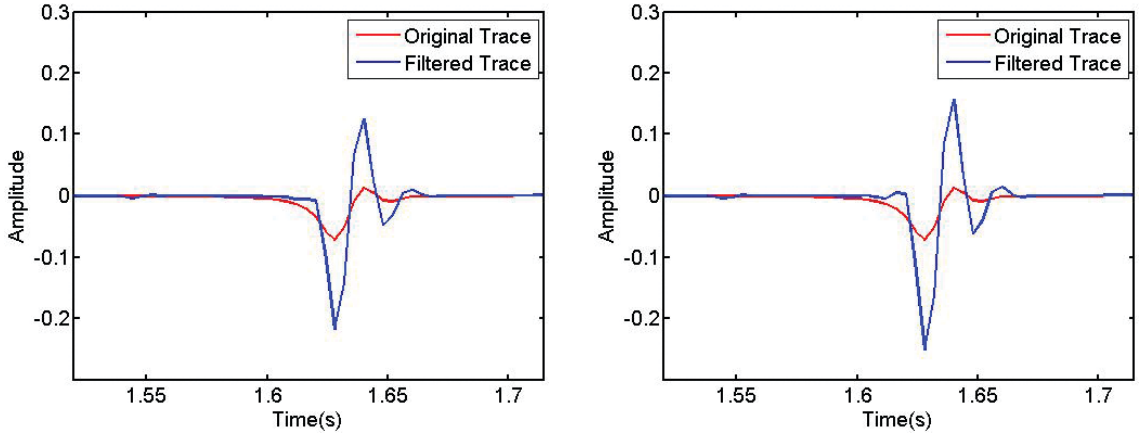

Figure 22 – Top of reservoir (Model 2): $Q_{ef} = 134.5$ (left) and $Q_{ave} = 117.0$ (right).

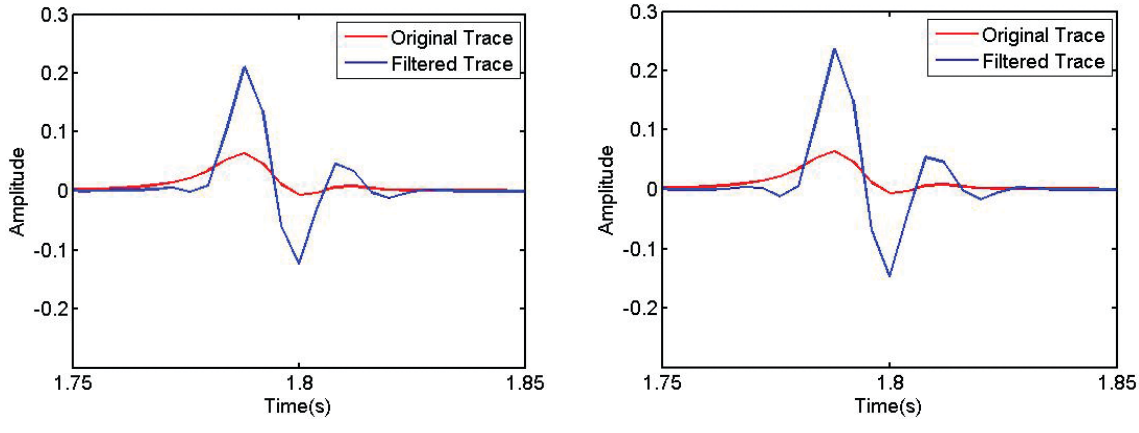

Figure 23 – Base of reservoir (Model 2): $Q_{ef} = 130.0$ (left) and $Q_{ave} = 117.0$ (right).

ACKNOWLEDGMENTS

The authors thank LENEP/UENF for the key-support regarding infrastructure, also the technicians Remilson Rosa and Adrielle Silva for their dedication in data acquisition, as well as Carlos A. Martins and Wagner Lupinacci for their support in the drafting of numerical simulation codes.

REFERENCES

AKI R & RICHARDS P. 1980. Quantitative Seismology: Theory and Methods, W.H. Freeman and Company, San Francisco, CA. 700 pp.

BARTON N. 2007. Rock Quality, Seismic Velocity, Attenuation and Anisotropy. Taylor & Francis Group, London, UK. 729 pp.

BATH M. 1974. Spectral analysis in geophysics. In: BATH M (Ed.). Developments in Solid Earth Geophysics. Vol. 7. Elsevier Science Publishing Co. 563 pp.

BLIAS E. 2012. Accurate Interval Q-Factor Estimation From VSP Data. Geophysics, Vol. 77, No. 3. May-June 2012; P. WA 149-WA 156.

CARCIONE J & PICOTTI S. 2006. P-Wave Seismic Attenuation by Slow-Wave Diffusion: Effects of Inhomogeneous Rock Properties. Geophysics, 71(3): 1–8.

CASTAGNA JLP, SUN S & SIEGFRIELD RW. 2003. Instantaneous spectral analysis. Detection of low-frequency shadows associated with hydrocarbons. The Leading Edge, 22(2): 120–127.

CHOPRA S, ALEXEEV V, MANERIKAR A & KRYSAN A. 2004. Processing Integration of Simultaneously Acquired 3D surface Seismic and 3D VSP Data. The Leading Edge, 422–430.

GUERRA R & LEANEY S. 2006. $Q(z)$ Model Building Using Walkaway VSP Data. Geophysics, 71(5): V127–V132.

HARDAGE BA. 2000. Vertical Seismic Profiling: Principles. Handbook of Geophysical Exploration. Seismic Exploration. Third update and revised edition, USA. 572 pp.

HARGREAVES ND & CALVERT AJ. 1991. Inverse Q Filtering by Fourier Transform. Geophysics, 56(4): April; P519–527.

KJARTANSSON E. 1979. Constant Q-wave propagation and attenuation. Journal of Geophysical Research, 84: 4737–4748.

MATSUMURA CN. 2006. Modelagem Acústica, Elástica e Viscoelástica. Aplicações na Geofísica de Reservatórios. Tese de Doutorado. LENEP/UENF. Brasil. 176 pp.

PICOTTI S, CARCIONE JM, RUBINO G & SANTOS JE. 2007. P-wave seismic attenuation by slow-wave diffusion. Numerical experiments in partially saturated rocks. Geophysics, 72(4): 11–21.

QUINTAL B, SCHMALHOLZ SM & PODLADCHIKOV YY. 2011. Impact of fluid on the reflection coefficient of a poroelastic layer. Geophysics, 76(2): N1–N12.

QUINTAL B, SCHMALHOLZ SM & PODLADCHIKOV YY. 2009. Low-frequency reflections from a thin layer with high attenuation caused by interlayer flow. Geophysics, 74(1): N15–N23.

RAJI WO & RIETBROCK A. 2011. Enhanced Seismic Q compensation. SEG Annual Meeting. San Antonio.

REINE C, CLARCK R & BAAN M. 2012. Robust Prestack Q-Determination Using surface Seismic Data: Part 1 – Method and Synthetic Examples. Geophysics, 77(1): January-February; P. R45–R56.

TONN R. 1991. Determination of the seismic quality factor Q data: a comparison of different computational methods. Geophysical Prospecting, 39: 1–27.

WANG Y. 2002. A stable and efficient approach of inverse Q filtering. Geophysics, 67: 657–663.

YANG S & GAO J. 2010. Seismic Attenuation Estimation From Instantaneous Frequency. IEEE Geoscience and Remote Sensing letters, 7(1): 113–117.

YANG Y, LI Y & LIU T. 2009. 1D Viscoelastic waveform inversion for Q structures from the surface seismic and zero-offset VSP data. Geophysics, 74(6): 141–148.

YILMAZ O. 2001. Seismic Data Analysis: Processing, Inversion and Interpretation of Seismic Data. 2nd ed. Society of Exploration Geophysics,Tulsa, Oklahoma. V1-V2, 2027 p.

Recebido em 31 outubro, 2012 / Aceito em 26 setembro, 2013
Received on October 31, 2012 / Accepted on September 26, 2013

NOTES ABOUT THE AUTHORS

Adalto Oliveira da Silva graduated in Mathematics from Universidade Federal Fluminense (UFF). Holds a Master's degree in Computational Modelling at the Universidade do Estado do Rio de Janeiro (UERJ) and Doctoral degree in Reservoir and Exploration Engineering in the applied geophysics field at LENEP/UENF. Worked as Substitute Teacher in the Department of Mathematics of UFF and currently is professor at SEEDUC/RJ and the Faculdade Cenecista de Rio das Ostras (FACRO-CNEC) in the Production Engineering course. Areas of interest: seismic data processing, reservoir characterization.

Roseane Marchezi Misságia holds a civil engineering degree from the Universidade Católica de Minas Gerais – PUC, Belo Horizonte, Brazil, in 1985. Obtained a Master's degree in 1988 and a Ph.D. in 2003, in Exploration and Reservoir Engineering in the area of applied geophysics from LENEP/UENF. Currently, works as Associate Professor of Petrophysics at LENEP/UENF. Areas of interest: seismic data processing, characterization of physical and mechanical properties of rocks.

Marco Antonio Rodrigues Ceia holds a BS in Physics from the Universidade Federal do Rio de Janeiro (UFRJ). Obtained a M.Sc. degree in Geophysics at the MCT-Observatório Nacional and Ph.D. in Exploration and Reservoir Engineering in the area of applied geophysics at LENEP/UENF. Currently, works as Associate Professor of Petrophysics at LENEP/UENF. Areas of Interest: Physics of rocks, characterization of physical and mechanical properties of rocks and seismic data processing.